

Supporting Information

Delivery of Anti-miR-712 to Inflamed Endothelial Cells Using pBAE Nanoparticles Conjugated with VCAM-1 Targeting Peptide

Pere Dosta, Ian Tamargo, Victor Ramos, Sandeep Kumar¹, Dong Won Kang¹, Salvador Borrós, Hanjoong Jo**

1. Synthesis of pBAE polymers

Synthesis of poly(β -amino ester)s (pBAEs) was performed via a two-step procedure, as previously described.^[1] First, addition reaction of primary amines to an excess of diacrylates was used to synthesize an acrylate-terminated polymer (termed C6 polymer). Second, C6 polymer was end-capped with different thiol-terminated oligopeptides composed of Cys + 3 amino acids (Arg, Lys, His, Asp, or Glu). Synthesized structures were characterized by ¹H-NMR, recorded in a 400 MHz Varian (NMR Instruments, Clarendon Hills, IL). The molecular weight of C6 polymer was determined by HPLC.

C6 Polymer

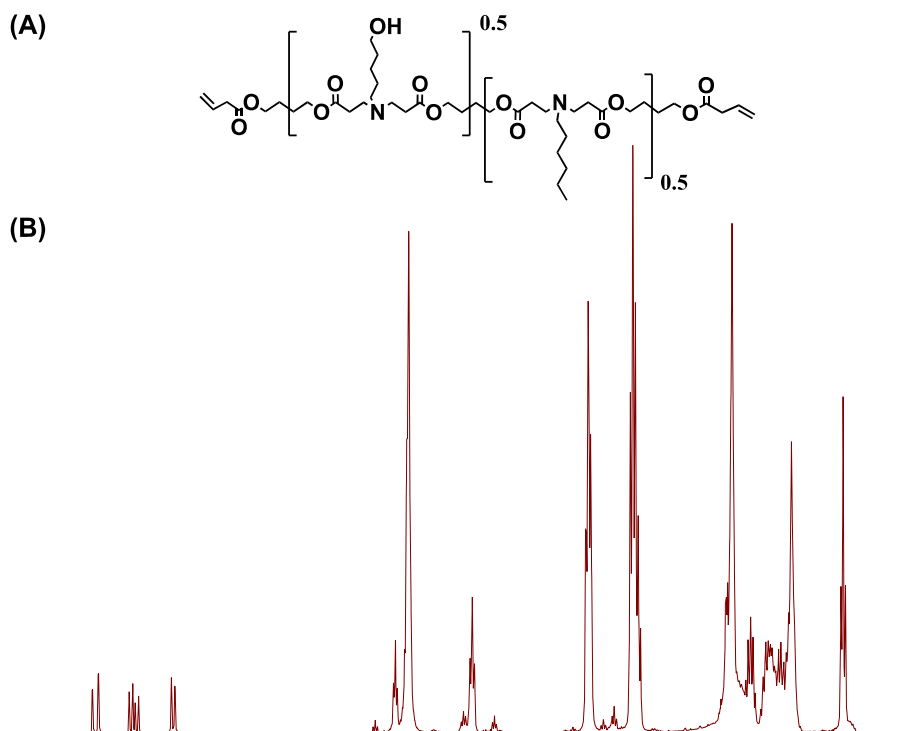


Figure S1: (A) Chemical structure of C6 polymer. (B) $^1\text{H-NMR}$ of C6 polymer.

$^1\text{H-NMR}$ (400MHz, Chloroform-*d*, TMS) (ppm): δ =6,41 (d, $\text{CH}_2=\text{CH-}$), 6,15 (d, $\text{CH}_2=\text{CH-}$), 5,87 (d, $\text{CH}_2=\text{CH-}$), 4,21 (br, $\text{CH}_2\text{-O-C(=O)-CH=CH}_2$), 4,11 (t, $-\text{CH}_2\text{-CH}_2\text{-O-}$), 3,64 (t, $\text{CH}_2\text{-CH}_2\text{-OH}$), 2,79 (br, $-\text{CH}_2\text{-CH}_2\text{-N-}$), 2,46 (br, $-\text{N-CH}_2\text{-CH}_2\text{-C(=O)-O}$), 1,83 - 1,60 (br, $-\text{O-CH}_2\text{-CH}_2\text{-CH}_2\text{-CH}_2\text{-O}$), 1,40- 1,18 (br, $-\text{CH}_2\text{-CH}_2\text{-CH}_2\text{-CH}_2\text{-OH}$, $\text{N-(CH}_2)_2\text{-CH}_2\text{-(CH}_2)_2\text{-OH}$), 0,90 (t, $\text{CH}_2\text{-CH}_2\text{-CH}_3$).

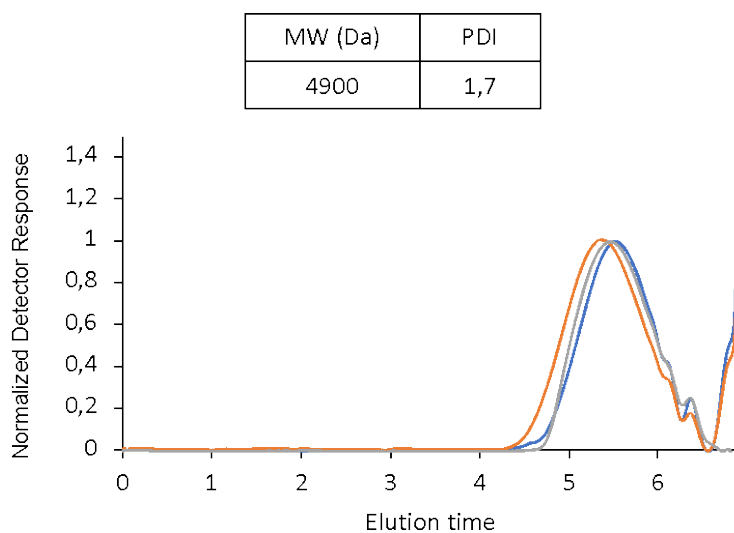


Figure S2: Molecular weight of C6 Polymer was determined by HPLC.

C6-CR3 Polymer

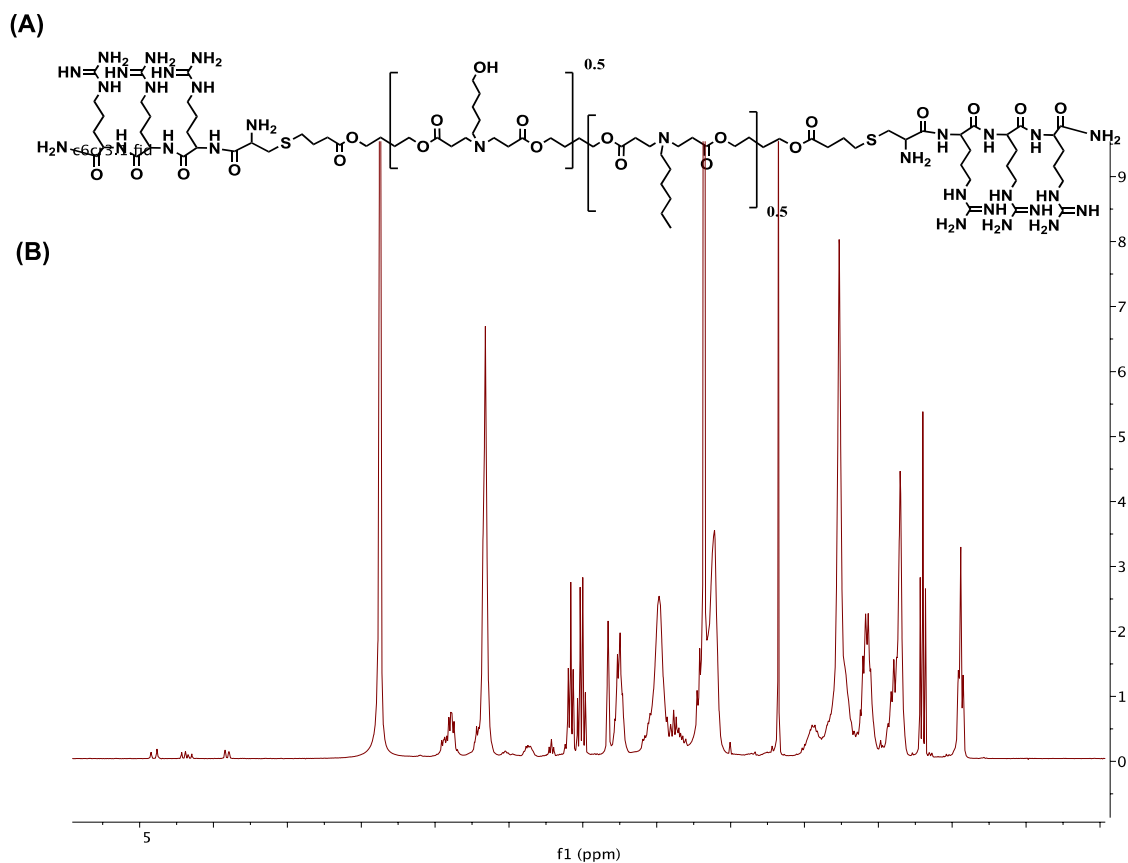


Figure S3: (A) Chemical structure of C6-CR3 polymer. (B) $^1\text{H-NMR}$ of C6-CR3 polymer.

$^1\text{H-NMR}$ (400MHz, Methanol- d_4 , TMS) (ppm): $\delta = 4.41\text{-}4.33$ (br, $\text{NH}_2\text{-C(=O)-CH-NH-C(=O)-CH-NH-C(=O)-CH-NH-C(=O)-CH-CH}_2\text{-}$), 4.16 (t, $\text{CH}_2\text{-CH}_2\text{-O}$), 3.58 (t, $\text{CH}_2\text{-CH}_2\text{-OH}$), 3.25 (br, $\text{NH}_2\text{-C(=NH)-NH-CH}_2\text{-}$, $\text{OH-(CH}_2\text{)}_4\text{-CH}_2\text{-N-}$), 3.04 (t, $\text{CH}_2\text{-CH}_2\text{-N-}$), 2.82 (dd, $\text{-CH}_2\text{-S-CH}_2\text{-}$), 2.48 (br, $\text{-N-CH}_2\text{-CH}_2\text{-C(=O)-O}$), 1.90 (m, $\text{NH}_2\text{-C(=NH)-NH-(CH}_2\text{)}_2\text{-CH}_2\text{-CH-}$), 1.73 (br, $\text{-O-CH}_2\text{-CH}_2\text{-CH}_2\text{-CH}_2\text{-O}$), 1.69 (m, $\text{NH}_2\text{-C(=NH)-NH-CH}_2\text{-CH}_2\text{-CH}_2\text{-}$), 1.56 (br, $\text{-CH}_2\text{-CH}_2\text{-CH}_2\text{-CH}_2\text{-OH}$), 1.39 (br, $\text{-N-(CH}_2\text{)}_2\text{-CH}_2\text{-(CH}_2\text{)}_2\text{-OH}$), 0.88 (t, $\text{CH}_2\text{-CH}_2\text{-CH}_3$).

C6-CK3 Polymer

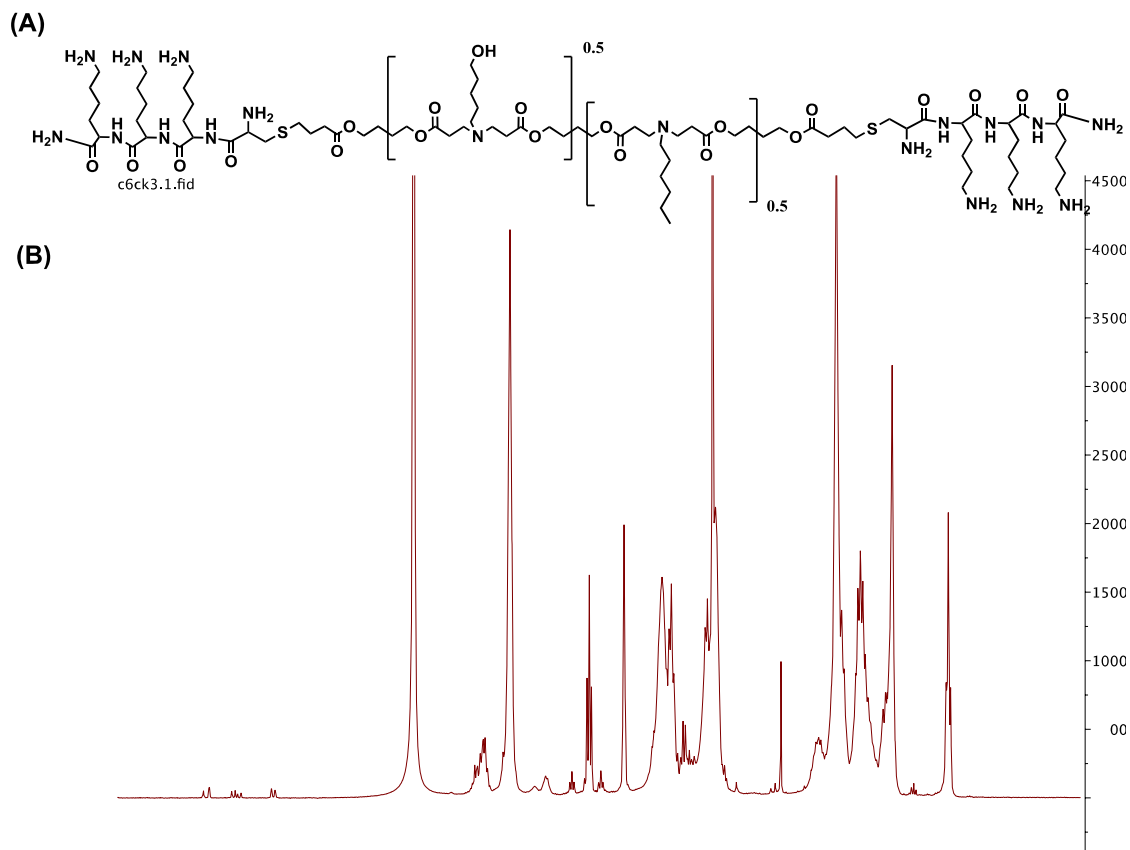


Figure S4: (A) Chemical structure of C6-CK3 polymer. (B) ¹H-NMR of C6-CK3 polymer.

¹H-NMR (400MHz, Methanol-*d*₄, TMS) (ppm): δ = 4.38-4.29 (br, NH₂-(CH₂)₄-CH-), 4.13 (t, CH₂-CH₂-O-), 3.73 (br, NH₂-CH-CH₂-S-), 3.55 (t, CH₂-CH₂-OH), 2.94 (br, CH₂-CH₂-N-, NH₂-CH₂-(CH₂)₃-CH-), 2.81 (dd, -CH₂-S-CH₂), 2.57 (br, -N-CH₂-CH₂-C(=O)-O), 1.85 (m, NH₂-(CH₂)₃-CH₂-CH-), 1.74 (br, -O-CH₂-CH₂-CH₂-CH₂-O), 1.68 (m, NH₂-CH₂-CH₂-(CH₂)₂-CH-), 1.54 (br, -CH₂-CH₂-CH₂-CH₂-OH), 1.37 (br, N-(CH₂)₂-CH₂-(CH₂)₂-OH), 0.88 (t, CH₂-CH₂-CH₃).

C6-CH3 Polymer

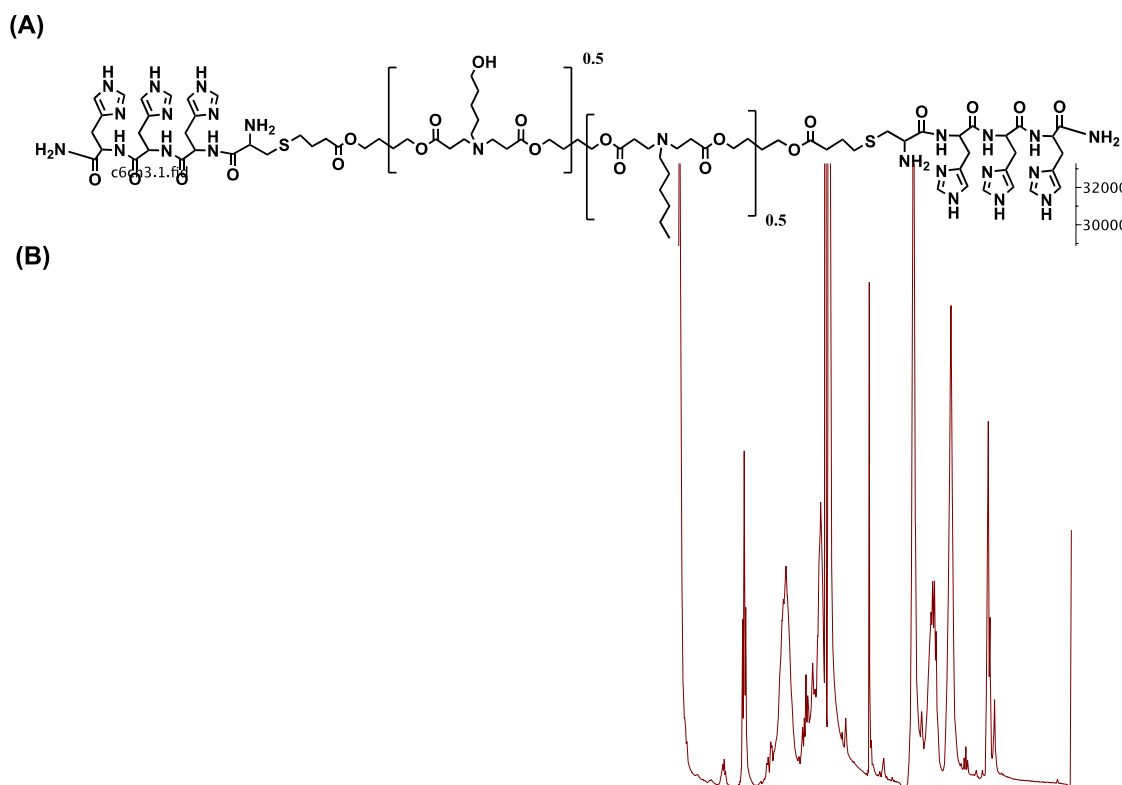


Figure S5: (A) Chemical structure of C6-CH3 polymer. (B) ¹H-NMR of C6-CH3 polymer.

¹H-NMR (400MHz, Methanol-*d*₄, TMS) (ppm): δ = 8.0-7.0 (br -N(=CH)-NH-C(=CH)-), 4.61-4.36 (br, -CH₂-CH-), 4.16 (t, CH₂-CH₂-O-), 3.55 (t, CH₂-CH₂-OH), 3.18 (t, CH₂-CH₂-N-), 3.06 (dd, -CH₂-CH-), 2.88 (br, OH-(CH₂)₄-CH₂-N-), 2.82 (dd, -CH₂-S-CH₂-), 2.72 (br, -N-CH₂-CH₂-C(=O)-O), 1.75 (br, -O-CH₂-CH₂-CH₂-CH₂-O), 1.65 (m, NH₂-CH₂-CH₂-(CH₂)₂-CH-), 1.58 (br, -CH₂-CH₂-CH₂-CH₂-OH), 1.40 (br, N-(CH₂)₂-CH₂-(CH₂)₂-OH), 0.88 (t, CH₂-CH₂-CH₃).

C6-CD3 Polymer

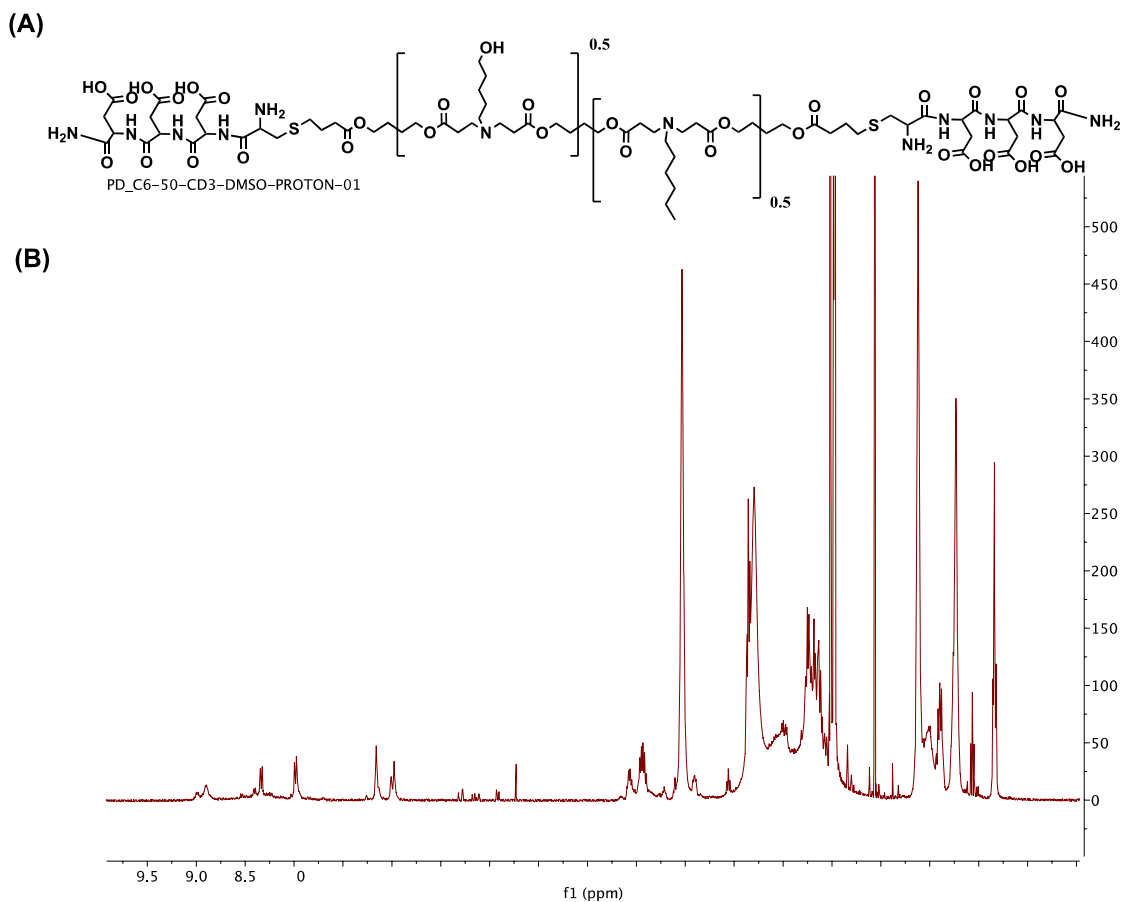


Figure S6: (A) Chemical structure of C6-CD3 polymer. (B) ¹H-NMR of C6-CD3 polymer.

¹H-NMR (400MHz, DMSO-*d*₆, TMS) (ppm): $\delta = 4.56-4.44$ (br, NH₂-C(=O)-CH-NH-C(=O)-CH-NH-C(=O)-CH-NH-C(=O)-CH-CH₂-), 4.19 (br, NH₂-CH-CH₂-S), 4.00 (t, CH₂-CH₂-O), 3.34 (t, CH₂-CH₂-OH), 2.98 (dd, -CH₂-S-CH₂), 2.57-2.48 (t, -CH-CH₂-COO-), 2.40 (br, -N-CH₂-CH₂-C(=O)-O), 1.60 (br, -O-CH₂-CH₂-CH₂-CH₂-O), 1.38 (br, -CH₂-CH₂-CH₂-CH₂-OH), 1.20 (br, -N-(CH₂)₂-CH₂-(CH₂)₂-OH), 0.88 (t, CH₂-CH₂-CH₃).

2. Synthesis of HPMA monomer

N-(2-hydroxypropyl)methacrylamide (HPMA) monomer was synthesized by acylation of 1-aminopropan-2-ol with methacryloyl chloride using anhydrous sodium hydrogen carbonate (NaHCO₃). NaHCO₃ was used as a base to quench HCl byproduct obtained during the HPMA synthesis. The

reaction was stirred in order to ensure that the two phases formed by NaHCO₃ and organic DCM solvent were vigorously mixed. The reaction was carried out at -20 °C and the final product was recrystallized from Et₂O:MeOH (3:1). The chemical structure analyzed by ¹H-NMR was in concordance with the previously described HPMA structure.^[2]



Figure S7: Synthesis of HPMA monomer.

¹H-NMR (200 MHz, CDCl₃, TMS) (ppm): δ = 6.63 (s, 1H, NH), 5.71 (s, 1H, H- 3ii), 5.32 (t, 1H, H- 3i), 3.91 (m, 1H, H-6), 3.70 (d, 1H, OH), 3.46 (dq, 1H), 3.13 (m, 1H), 1.94 (s, 3H, H-1), 1.16 (d, 3H, H- 7)

IR (ATIR) ν = 659, 824, 845, 914, 1001, 1053, 1088, 1117, 1142, 1232, 1263, 1331, 1427, 1553, 1614, 1653, 2933, 2976, 3275, 3306 cm⁻¹

3. Synthesis of Ma-acap-TT monomer

Ma-acap-TT monomer was synthesized in two steps. First, Ma-acap-OH intermediate was obtained by acylation of aminocaproic acid with methacryloyl chloride in aqueous NaOH, in a procedure known as the Schotten-Baumann reaction (highly exothermic reaction). Then, Ma-acap-OH was recrystallized twice using EtOAc:Et₂O. The intermediate Ma-acap-OH chemical composition was confirmed by ¹H-NMR and the results were in concordance with with previously described Ma-acap-OH structure by Šubr and colleagues.^[3]

Once Ma-acap-OH intermediate was synthesized, Ma-acap-TT was obtained by acylation of 2-thiazoline-2-thiol (TT) with the free carboxylic group of Ma-acap-OH using dicyclohexylcarbodiimide (DCC) and a catalytic amount of 4-dimethyl-aminopyridine (DMAP) in THF. The reaction was confirmed by the formation of white crystalline precipitate N,N'-dicyclohexylurea salt (DCU). Then, DCU salt was removed by filtration and the final product was recrystallized using ethanol. Chemical structure analysed by $^1\text{H-NMR}$ was in concordance with previously described HPMA structure.^[3]

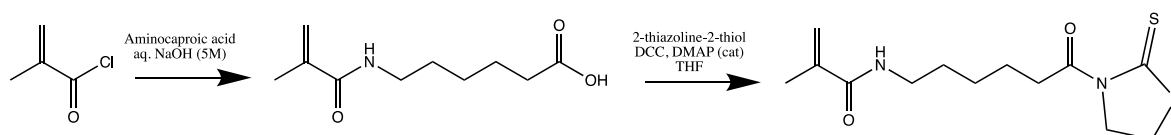


Figure S8: Synthesis of Ma-acap-TT monomer.

$^1\text{H-NMR}$ (200 MHz, CDCl_3 , TMS) (ppm): $\delta = 5.86$ (s, 1H, NH), 5.67 (s, 1H, H-3ii), 5.31 (t, 1H, H-3i), 4.58 (t, 2H, H-13), 3.29 (m, 6H, H-5, H-9, H-12), 1.97 (s, 3H, H-1), 1.80 – 1.30 (m, 6H, H-6 H-7 H-8)

IR (ATIR) $\nu = 677, 717, 878, 933, 1005, 1039, 1150, 1232, 1279, 1356, 1387, 1549, 1605, 1651, 1697, 2855, 2930, 3284 \text{ cm}^{-1}$

4. Synthesis of pHPMA-TT copolymers

HPMA (3.0 g, 20.9 mmol), Ma-acap-TT (0.7 g, 2.3 mmol), and AIBN (0.59 g, 3.6 mmol) were dissolved in dry DMSO (25.3 g, 17.1 mL), and allowed to polymerize by reversible addition-fragmentation chain transfer (RAFT) reactions at 60 °C for 6 hours under inert atmosphere. The presence of TT groups was confirmed by $^1\text{H-NMR}$.

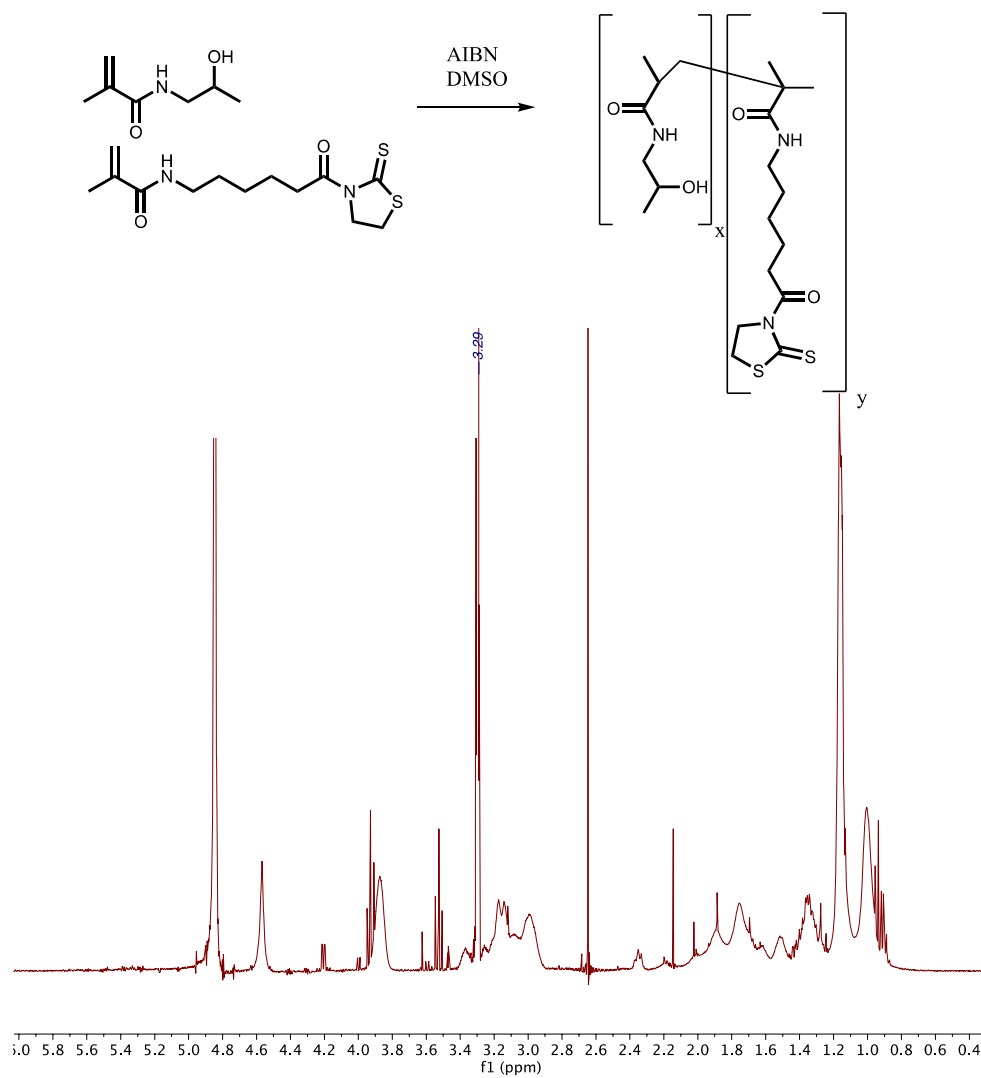


Figure S9: (A) Chemical structure of pHPMA-TT polymer. (B) $^1\text{H-NMR}$ of pHPMA-TT polymer.

5. Synthesis of pHPMA-TT-Mal copolymer

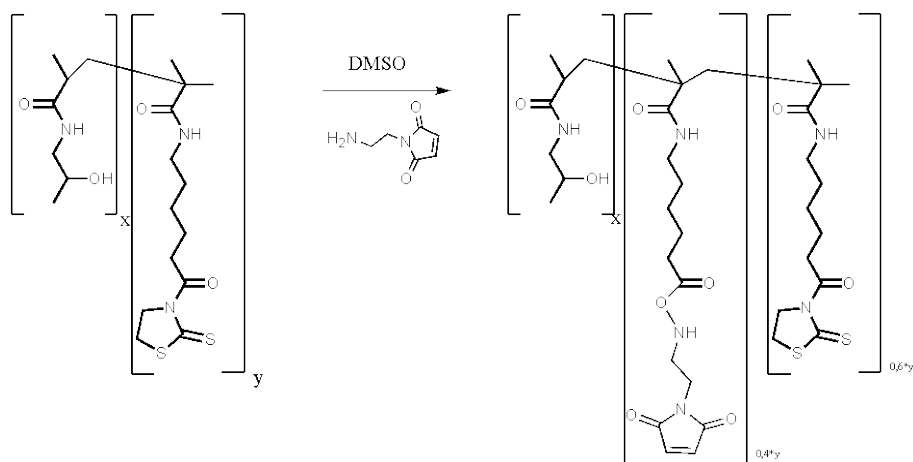


Figure S10: Synthesis of pHPMA-TT-Mal polymer. 40% of TT-group from pHPMA-TT copolymer were modified using amino-maleimide.

6. Characterization of VHPK-targeted NPs.

(A)

	DLS			NTA
	Size (nm)	Z-Pot (mV)	PDI	Size (nm)
pBAE NP	70.0 ± 1.3	21.5 ± 1.0	0.124 ± 0.061	74.6 ± 18.6
c-pBAE NP	93.4 ± 3.8	6.0 ± 1.0	0.131 ± 0.081	108.7 ± 36.3
VHPK-c-pBAE NP	100.8 ± 2.1	8.1 ± 0.9	0.158 ± 0.107	126 ± 57.0

(B)

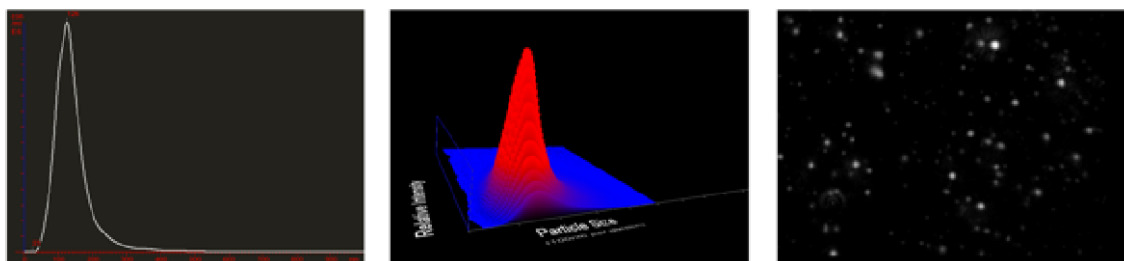


Figure S11: Characterization of VHPK-targeted NPs. (A) Hydrodynamic size, zeta-potential (Z-Pot), and Polydispersity (PDI) of coated and non-coated pBAE NPs, and targeted and non-targeted pBAE NPs were determined by Dynamic Light Scattering (DLS) and Nanoparticle Tracking Analysis (NTA). Results are shown as the mean \pm s.e.m of triplicates. (B) Size distribution (left), bimodal distribution size-polydispersity (middle), and nanoparticle image (right) was determined by Nanoparticle Tracking Analysis.

7. pHPMA coating optimization in C6-KH nanoparticles

Different pHPMA copolymer quantities were combined with the pBAE NPs in order to determine the optimal pHPMA/pBAE NP ratio (ranging from 3.12% to 50% w/w). NP synthesis was carried out as previously described, and their ability to deliver anti-miR-Cy3 was tested by flow cytometry.

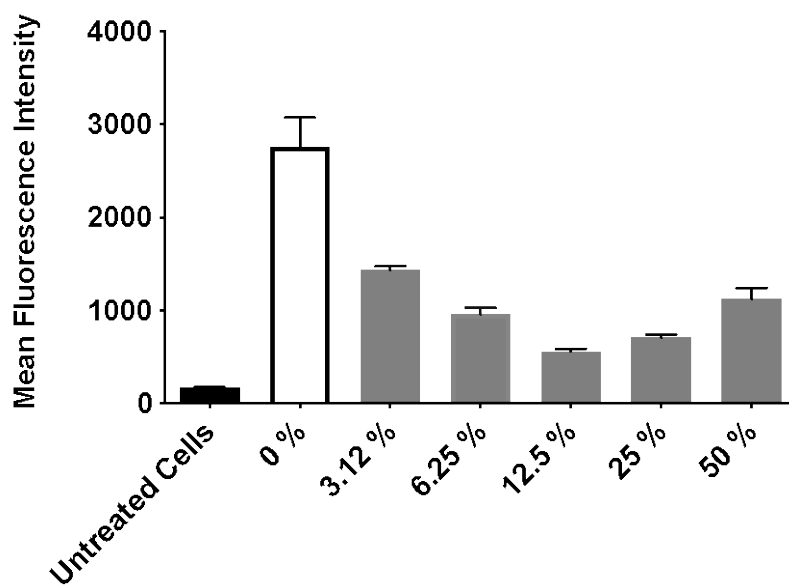


Figure S12: pHPMA coating optimization in C6-KH nanoparticles. Different pHPMA coating percentages were added over C6-KH pBAE NPs containing anti-miRNA-Cy3, ranging from 0 to 50% w/w. Their uptake efficiencies were analyzed by flow cytometry in iMAECs. Data are represented as mean \pm SEM (n = 3).

8. Non-selective uptake of VHPK-c-pBAE NPs in healthy iMAECs

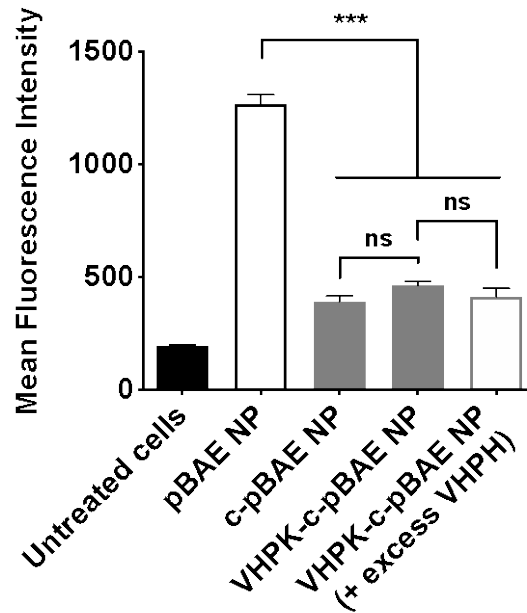


Figure S13: Non-selective uptake of VHPK-c-pBAE NPs in healthy iMAECs. pBAE NPs containing anti-miR-Cy3 were coated with pHPMA-TT polymer (c-pBAE NP) and conjugated with VHPK peptide (VHPK-c-pBAE NP). Internalization efficiency was tested at 2 hours post-transfection using healthy iMAECs by flow cytometry. To assess VHPK-mediated internalization, the VCAM-1 receptor in healthy iMAECs was blocked using excess VHPK peptide. Data are represented as mean \pm SEM (n = 3). Multiple comparisons among groups were determined using one-way ANOVA followed by a post-hoc test. *P*-value: **p* < 0.05, ***p* < 0.01, ****p* < 0.001.

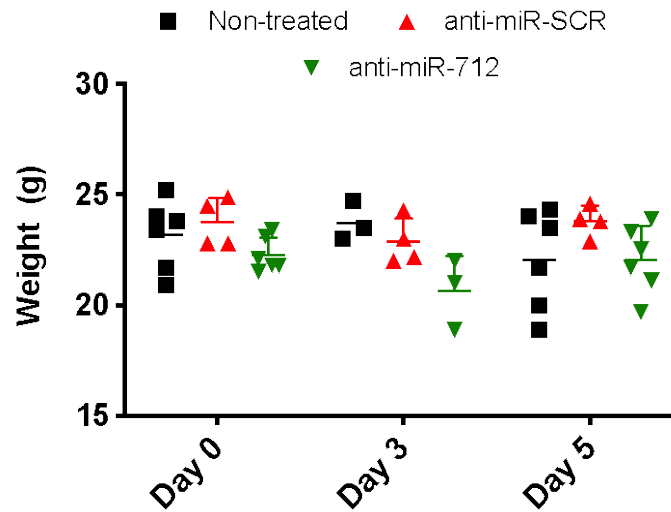


Figure S14: Mice weight monitoring after anti-miR-712 and anti-miR-SCR injection using VHPK-c-pBAE NP at 1 mg kg^{-1} . $n = 5$, data shown as mean \pm s.e.m.

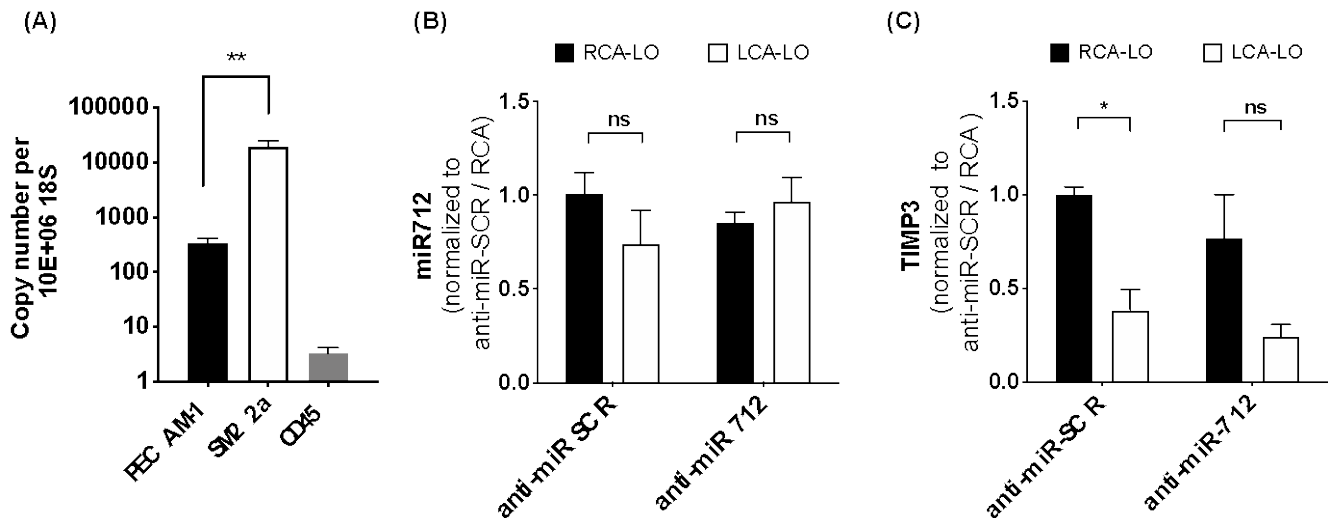


Figure S15: (A) Quality criteria of leftover (LO) smooth muscle cell-enriched layer was determined by analyzing PECAM-1 as an endothelial marker, SM22a as a smooth muscle cell marker and CD45 as an immune cell marker. Statistical significance was analyzed between PECAM-1 and SM22a markers. (B) miR-712 and (C) TIMP3 expression was analyzed in LO smooth muscle cell-enriched samples from RCA and LCA at 48 hours post-injection in PCL mice model. Data are represented as mean \pm SEM (n

= 4-6). Pairwise comparisons were determined using Student t-tests. P-value: *p < 0.05, **p < 0.01, ***p < 0.001.

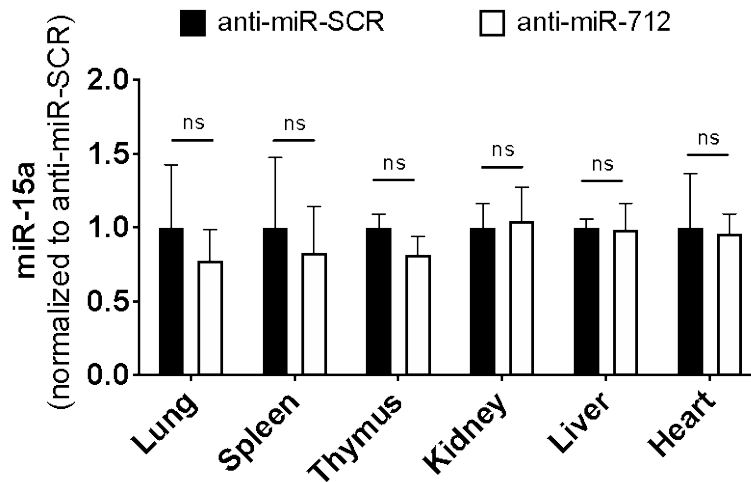


Figure S16: miR-15a quantification in anti-miR-712 biodistribution study. Data are represented as mean ± SEM (n = 5). Pairwise comparisons were determined using Student t-tests. P-value: *p < 0.05, **p < 0.01, ***p < 0.001.

Primer	Forward Sequence	Reverse Sequence
18S	5'-AGGAATTGACGGAAGGGCACCA-3'	5'-GTGCAGCCCCGACATCTAAG-3'
mPECAM1	5'-GCTGGTGCTCTATGCAAGC-3'	5'-ATGGATGCTGTTGATGGTGA-3'
mSM22a	5'-CCTTCCAGTCCACAAACGAC-3'	5'-GTAGGATGGACCCTTGTGG-3'
mCD45	5'-CTTCAGTGGTCCCATTGTGGTG-3'	5'-TCAGACACCTCTGTCGCCTTAG-3'
mTIMP3	5'-CACGGAAGCCTCTGAAAGTC-3'	5'-TCCCACCTCTCCACAAAGTT-3'
mIL6	5'-TCCTCTGTGAAGTCTCCTCTCCGG-3'	5'-TGGGACTGATGCTGGTGACAACCA-3'
mVCAM1	5'-GCTATGAGGATGGAAGACTCTGG-3'	5'-ACTTGTGCAGCCACCTGAGATC-3'
mTNF- α	5'-TGCTGGGAAGCCTAAAAG-3'	5'-CGAATTTGAGAAGATGATCCTG-3'

Table S1: Primers sequences used for qPCR analysis.

References

- [1] P. Dosta, V. Ramos, S. Borrós, *Mol. Syst. Des. Eng.* **2018**, 3, 677.
- [2] K. Ulbrich, V. Subr, J. Strohalm, D. Plocova, M. Jelinkova, B. Rihova, *J Control Release* **2000**, 64, 63.
- [3] V. U. Šubr, K., *React. Funct. Polym.* **2006**, 66, 1525.